Mapana – Journal of Sciences
2024, Vol. 23, No. 1, 93-117
ISSN 0975-3303|https://doi.org/10.12723/mjs.68.5

Enhanced Nickel Removal from Aqueous Solutions using Chemically Modified Tabeuaba Rosea Leaves as Biosorbent

Pranali I. Choudhari*, Sarang S. Dhote* and Mamata R. Lanjewar†

Abstract

The current study explored batch testing to adsorb Ni(II) onto Tabeubea rosea leaves activated by zinc chloride (TRZCAC), assessing parameters like contact time, pH, adsorbent amount, initial metal ion concentration, and temperature. Characterization via BET, FTIR, SEM, EDX, and TGA analyses revealed TRZCAC's surface area (693.113 m^2/g) and morphology. Optimal conditions were determined as pH 6, 0.5g adsorbent dose, 120 min adsorption time, and 50 mg L^{-1} Ni(II) concentration, yielding a 91.29% removal and 22.47 mg/g adsorption capacity. Pseudo-second-order kinetics described adsorption, which was spontaneous and exothermic. Freundlich isotherm and second-order kinetics best fit the data. The findings suggest TRZCAC as a potential eco-friendly biosorbent for Ni(II) removal from wastewater, owing to its effective adsorption capacity and favorable operating conditions.

Keywords: Adsorption, Adsorption isotherm, Adsorption kinetics, Ni (II), Tabeubea rosea leaves, $ZnCl_2$

---

* Shri Shivaji Education Society Amravati's Science College, Nagpur-440033, Maharashtra, India; pranalichoudhari21@gmail.com *(Corresponding author)*; sarangdhote@gmail.com

† Post Graduate Teaching Department of Chemistry, R.T.M. Nagpur University, Nagpur-440033, Maharashtra, India; mr_lanjewar@rediffmail.com

Highlights

- Tabeubea rosea Zinc chloride Activated carbon (TRZCAC) has been developed for the removal of Ni(II) metal ion from water.
- The TRZCAC's maximum surface area was determined to be 693.113 m^2/g.
- Excellent biomaterial for treatment that is also environmentally friendly.
- This is the first published work that uses TRZCAC to remove Ni(II) metal ions.

Introduction

Among the hazardous heavy metals found in wastewater that is not biodegradable is nickel. The waste products from industrial production operations like mining, painting, galvanizing, smelting, dye making, and metal finishing typically contain Nickel (Al-Qodah, 2006)]. According to WHO guidelines, the maximum amount of nickel that can be present in industrial wastewater is 2.0 mg/L and the range of Ni(II) concentration in industrial effluent is 3.40 to 900 mg/L (MINAS Pollution Control Acts 2001) So, before releasing industrial wastewater into the environment, it's crucial to remove Ni(II) from them. Renal cancer, non-cancerous toxicity effects after inhalation, dermatitis, and reproductive consequences are notable human health toxicity effects found in human and/or animal studies. The indirect genotoxic and epigenetic processes that underlie the threshold mode of action for nickel carcinogenicity are the sources of these effects' thresholds.(Buxton et al., 2019).The concentration threshold of nickel deemed harmful to human health are as follow NACD(human)-Dermal-NOAEL=0.44ug Ni/cm^2 skin/day(Fischer et al., 2005).Oral-BMDL$_{0.1=}$4.3 ug Ni/kg bw/day adult(in addition to diet)"(Haber et al., 2017).Respiratory cancer (human)-Inhalation practical threshold=0.1 mg Ni/m^3 inhalable aerosol(Oller et al., 2014). Inhalation practical threshold=0.5 mg Ni/m^3 PM10 aerosol (Buekers et al., 2015).

Several technologies, including coagulation, froth flotation, filtration, ion exchange, electrolytic precipitation solvent extraction, adsorption, electrolysis, reverse osmosis photocatalytic reduction methods are available to manage water pollution with varied degrees of success (Raval et al., 2016)(Rengaraj et al., 2003)(Hasija et al., 2021)(Y. C. Sharma et al., 2008)(Hariharan et al., 2023).However, because of their expensive cost, delicate working circumstances, and low removal efficiency, their usage is limited. Additionally, the most of them require multi-step processing.

Although there are many different nickel removal techniques, none of them are by themselves inexpensive, simple to use, or ecologically benign. The precipitation-coagulation method, for example, is simple to use but results in a lot of sludge that needs to be treated later, which raises disposal costs. In the dynamic presence of other competing metal ions, anion exchange processes exhibit relatively low selectivity (Biswas et al., 2008)(Tsuji, 2002). Reverse osmosis and ion exchange, while successful, are expensive because of high running and maintenance expenses throughout the course of their useful lives.

The biosorption process is convenient, simple to use, less expensive to operate. It is considered a desirable technology because, even at low concentrations, it is especially effective at eliminating heavy metals from diluted solutions. Agro-industrial waste products can remove heavy metals since they are inexpensive and readily available in large quantities. For the treatment of an aqueous solution of Ni(II), prospective biosorbents like non-living plant material, such as wood, roots, leaves, and bark (Vinod et al., 2010) and grape stalk villaiscusa (Villaescusa et al., 2004) debris, have recently been employed. The poisonous nature of nickel and its ability to cause human cancer make it a severe concern. Heart attacks, breathing issues, renal damage, and gastrointestinal upset are just a few of the diseases that nickel can cause (Bulgariu & Bulgariu, 2012). Since nickel contamination is a problem for the environment on a global scale, research has been done to create better and more efficient treatment methods to extract nickel ions and other hazardous metals from wastewater.

Adsorption removal can be an easy, economical, and environmentally beneficial technique, depending on the type of adsorbent used. As a result, it has been increasingly popular in recent years to use easily available and inexpensive waste materials as biosorbents to extract heavy metals in wastewater .Several waste materials-based biosorbents such as coconut husk, wheat and barly straw(Chand et al., 2009), orange peel (Akinhanmi et al., 2020), nutshells (Das et al., 2020), Moringa oleifera tree (Bello et al., 2017)], coffee husk(Alhogbi, 2017), coconut shell(Song et al., 2014), Imperata cylindrical waste leaf(Li et al., 2013), Pomegranate waste(Bellahsen et al., 2021), wild apple fruit dust(Pavlić et al., 2017), fig leaves(Gebreslassie, 2020), potato peel(El-Azazy et al., 2019), Rice husk(Ahmaruzzaman & Gupta, 2011) etc. The process of making activated carbon from raw date palm fronds by activating them with $ZnCl_2$ produced the product with the maximum surface area. (Ahmad et al., 2015). One promising low-cost biosorbent that works well for removing metals after being treated with $ZnCl_2$ is activated carbon derived from agricultural waste.

As evidenced by the studies cited above, no research has been done on synthesizing activated carbon from Tabeubea rosea leaves that are then chemically activated by ZnCl2.This allows us to use environmental waste and incorporate it into the economy. This work aims to synthesize activated carbon using ZnCl2, optimize the carbon by its surface area and pore volumes, and analyze it using FTIR, XRD, and TGA techniques. The unique aspect of this work is the use of mature Tabeubea rosea leaves, an eco-waste that is transformed into activated carbon using ZnCl2.

Experimental

Chemicals

Nickel sulfate, dimethylgyoxime, bromine water, and ammonia were brought from Merk, India.Aqueous solutions were prepared using double-distilled water. Since, all of the reagents were analytical grade, no further purification was needed.

Ni(II) Solution Preparation:

0.492 g of $NiSO_4$ were dissolved in 1000 ml of distilled water to create an aqueous stock solution with 100 mg/L of Nickel (II). After that, the stock solution was appropriately diluted with double-distilled water to obtain an appropriate Nickel (II) concentration.

Preparation of Tabeubea Rosea Zinc Chloride activated carbon (TRZCAC)

Tabeubea rosea Known by most as the "Pink Trumpet Tree," this tree is well-known for its exquisite blossoms. Tabeubea rosea belongs to kingdom-Plantae, division-Tracheophytes, subdivision-Angiosprin, class-Eudicots, Sub-class-Asterids, Order-Lamiales & family-Bignoniaceae.Mature Tabeubea rosea leaves were collected in Nagpur District, Maharashtra, India, from a nearby agricultural area. Tabeubea rosea mature leaves were thoroughly cleaned with double-distilled water before being crisp-dried for several days in the sun. Which had been then crushed using a crusher. Then, it is carbonized for two hours at 600^{0}C in a nitrogen environment. The crushed Tabeubea rosea powdered leaves were then activated by adding 1 M zinc chloride in a ratio of 1:1 for 3–4 days. The carboni-sed substance is then allowed to cool. & repeatedly cleaned with double-distilled water until the zinc content of the filtrate was neg- ative. Following a 35 mesh screen sieve, it is stored for later use in an airtight bottle.

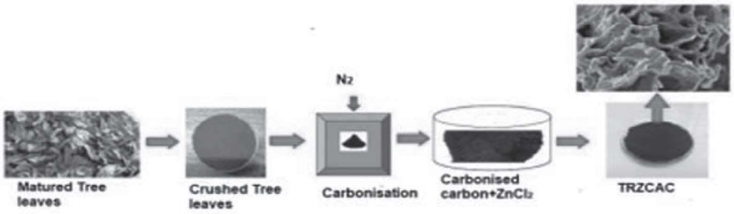

Schematic diagram for the Preparation of TRZCAC

Batch Adsorption Procedure:

The optimal conditions for the adsorption experiments, which used a range of Ni (II) concentrations between 10 mg/L and 100 mg/L, included maintaining the pH, adsorbent dosage, and adsorption time at room temperature (Kahu et al., 2016). At equilibrium, one can estimate the amount of Ni (II) adsorbed on TRZCAC.

$$q_e = \frac{C_i - C_e}{W} * V \quad (1)$$

Where,

C_0=Initial Ni (II) ion concentration

C_e=Equilibrium concentration of Ni (II) in mg/L

W= Weight of adsorbent in grams

V=Volume of Ni (II) solution in litres

To calculate the percentage of removal efficiency, the following formula was utilised.

$$\% \, Removal = \frac{C_i - C_e}{C_i} * 100 \qquad (2)$$

Result and Discussion:

Characterization of TRZCAC

In the adsorption experiment, the surface is the most crucial component.The nitrogen adsorption-desorption method at 77 K was used to calculate the BET surface area and pore volume of TRZCAC. The results showed that the pore volume and surface area were 3.94 cm3/g and 693.113 m2/g, respectively The multi point BET plot are shown in Fig 1. The FT-IR spectra for TRZCAC are shown in Fig 2. The complex character of the adsorbent made from Tabeubea rosea leaves activated with zinc chloride is demonstrated by the several absorption peaks visible in the FT-IR spectra. The peak at 3650cm-1 suggests O-H group stretching (Vithalkar et al., 2022). The -NH stretching is represented by the sharp peak at 3422 cm-1. The aliphatic C-H group could be associated with the band at 2930 cm-1. The peak at 2340 cm-1 is typically attributed to the $C\equiv C$ stretching vibration of alkyne groups. The signal at 1718 cm-1 indicates that a carbonyl (carboxylic) group may occur. The peak at 1500 cm-1 is associated with the N-H bending vibration. The broad peak at 1085 cm-1 indicates the presence of a phosphate functional group enhances the ability of adsorption (Lian et al., 2021). The morphological features of TRZCAC (surface texture and porosity), which are shown in Figs. 3(a)& 3(b), were ascertained by SEM. The figure depicts the biosorbent's internal microstructure and verifies that it has a well-defined porosity structure. In addition, the TRZCAC has an uneven surface with numerous tunnel-like structures. As seen in Fig. 4, tunnel-like structures observed in the material are beneficial for the adsorption of metal ions (Zhou et al., 2013).EDX was utilized to verify that components were present on the surface of TRZCAC. The contents of carbon, oxygen, and a few other elements were measured Fig 4(a). The principal and most frequently observed constituents in TRZCAC are carbon and oxygen contents. The weight loss of TRZCAC about temperature was measured using TGA. The sample shows three stages of weight loss with increasing temperature. The initial phase of weight loss, which happens between 100 and 2000C, is brought on by the loss of water and some light volatile substances.

At these temperatures, weight loss is approximately 3.03%. The second stage's temperature range extended from 250 to 600^0C, and a weight loss of roughly 5.91% was recorded. Above 200^0C is often when the lignocellulosic structure begins to decompose (A. Kumar et al., 2008). This was accompanied by an endotherm on the DTA curve. The conversion of hemicellulose and cellulose into gases and tars was the cause of the significant weight loss at this stage. Conversely, lignin underwent a slow conversion to fumes and tar. Furthermore, this phase initiates the carbon's creation. (Yang et al., 2007). Due to TRZCAC's carbon optimization, the third-step weight reduction steadily slowed down. According to the DTA curve, this breakdown is exothermic as depicted in **Figures 5(a) and 5(b).**

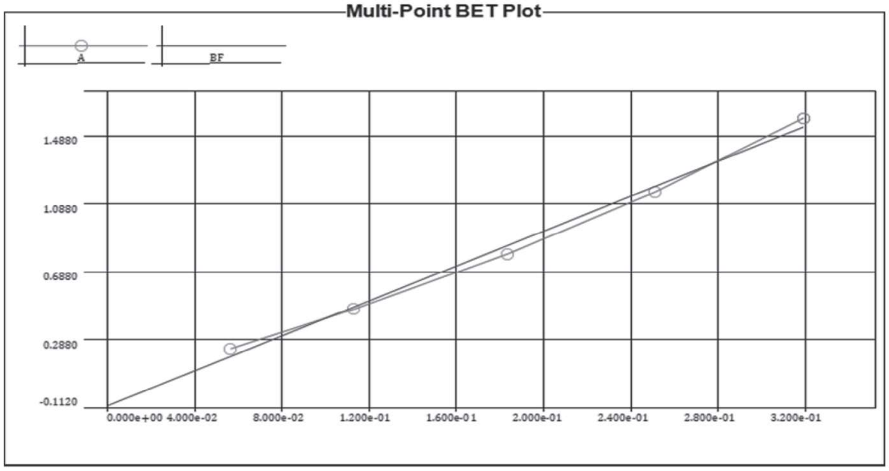

Fig.1 Multi point BET Plot

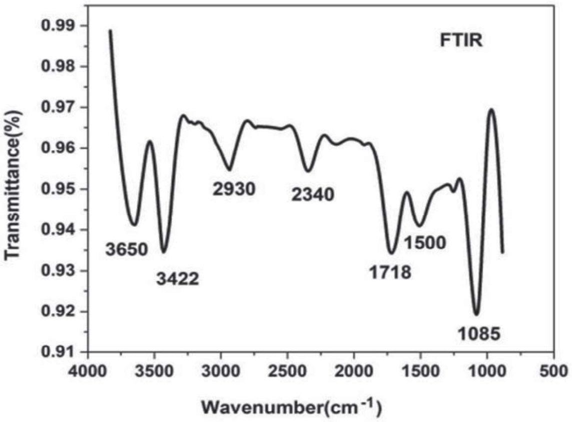

Fig.2 FTIR Spectra for TRZCAC

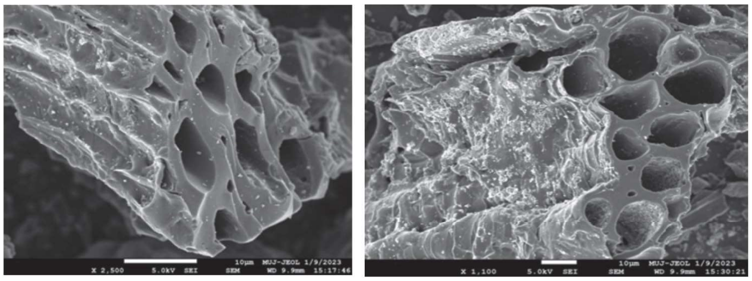

Fig.3(a) and 3(b) of SEM Images of TRZCAC

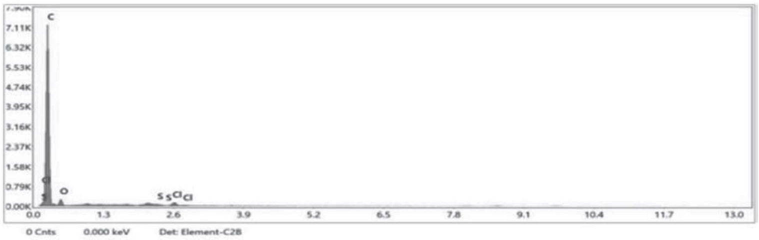

Fig.4 EDX Image of TRZCAC

Smart Quant Results

Element	Weight %	Atomic %	Error %
C K	88.1	91.4	4.7
O K	10.1	7.9	17.2
S K	0.9	0.4	8
ClK	0.9	0.3	8.9

Fig.4(a) Elemental Analysis

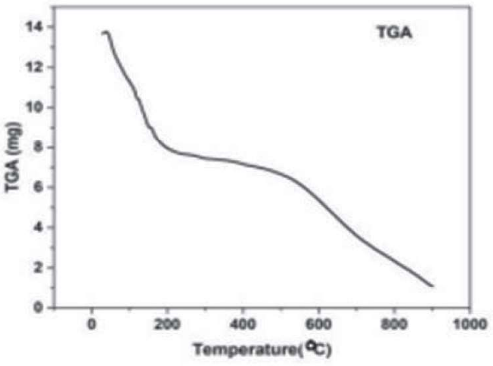

Fig.5(a) TGA curve of TRZCAC

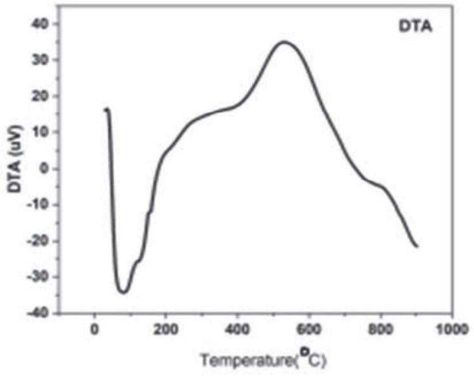

Fig.5(b) DTA curve of TRZCAC

Batch Adsorption Experiments:

Effect of pH_{PZC}

The point of zero charge (pHpzc) is an important metric.PZC value is used to determine a metal ion's capability for surface adsorption. (Mahmood et al., 2011). The salt addition method has been found appropriate and convenient to determine the pH_{PZC} of Ni(II)(Bakatula et al., 2018).To determine the pHpzc, it is ideal that the amount of positive and negative charges in the solid-liquid interface, represented by cations and anions, are equal. For this it is important that the ions are symmetrical in size, or of approximate sizes. In addition to good solubility in water, availability, relative low toxicity, sodium nitrate ions Na^+ and NO_3^- which both present an effective hydrated ionic radius

The evaluation was performed by mixing 0.5g of TRZCAC with 25 ml of several 0.1M $NaNO_3$ solutions having pH values between 1.0 and 12. After 24 hours of continuous shaking, the solutions were filtered, and their final pH was recorded. making a graph that compares the pH at the beginning and after the modification.

The graph's or the x-intercept's output was 6.0.

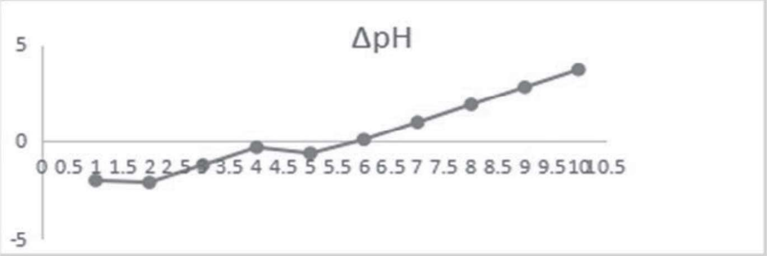

Fig.5(a). Effect Of p H$_{PZC}$

Effect of pH:

The ionization of the adsorption sites present on the surface of biosorbent particles is facilitated by the pH of the solution medium(Weber et al., 2013). Using 0.5 g of TRZCAC in a 100 ml solution, 120 minutes of shaking, and a 50 mg/L concentration of Ni(II) metal ions, the effects of pH were investigated.0.1 N HCl and 0.1 N NaOH solutions were used to increase the pH value from 3.0 to 12.0 (LIU et al., 2008).

Electrical repulsion among the H^+ ions and the metal cation on the surface of TRZCAC at lower pH reduced the positively charged adsorption sites and the metal's adsorption. Increased pH caused the TRZCAC surface to become more and more negatively charged, which speed up the adsorption of metal ions on the TRZCAC particles'surfaces (Sari et al., 2007; A. Sharma & Bhattacharyya, 2005) (Amode et al., 2016) At pH 6 metal ions were removed by 94.18% The metal ion become less stable as there is an increase in the solution pH and adsorption reaches equilibrium at 6.0. However, at still higher pH values there is a decrease in the removal of metal ion which is due to their precipitation of metal ion as their hydroxides (Fan et al., 2012).The investigation's findings imply that TRZCAC might work well as an adsorbent to remove metal ions.

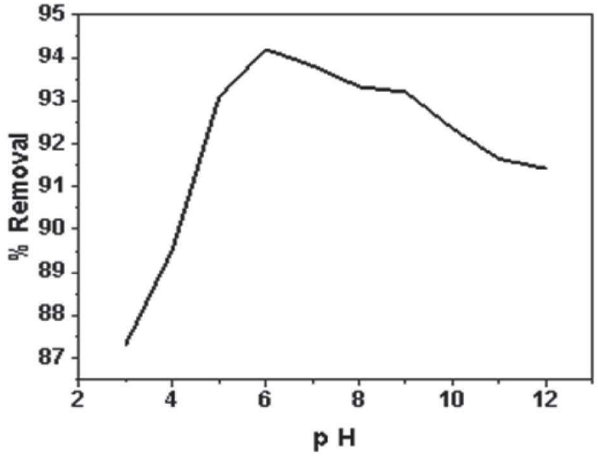

Fig.5(b). Effect of p H

Effect of Adsorbent Dosage

A 50 mg/L Ni(II) solution with different concentrations of TRZCAC could be used to determine the impact of adsorbent dosage on removal efficacy for 120 minutes at room temperature and optimum pH of 6.It can be demonstrated that the amount of Ni(II) removed increases from 0.1 to 1 gram of TRZCAC. The number of adsorption sites and surface area both increase with the degree of adsorption. The fraction of Ni(II) eliminated from the environment remained constant when equilibrium was reached.

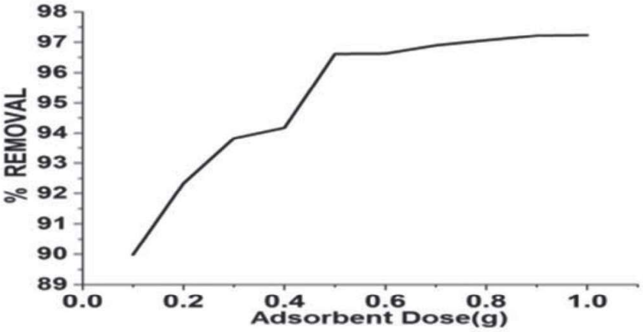

Fig.5(c): Effect of amount of adsorbent dosage

Effect of Contact Time:

To examine the effect of contact duration on the % removal of Ni(II) by TRZCAC, we employed an initial concentration of 0.5 g of adsorbent and a contact time range of 20-180 min. It was discovered that the maximum adsorption occurred after 120 minutes, and it was also discovered that Ni(II) removal effectiveness increased with the initial extension of contact time. As the contact period rises, the adsorption sites on the surface of TRZCAC become more readily available, causing them to become Ni(II)-loaded.

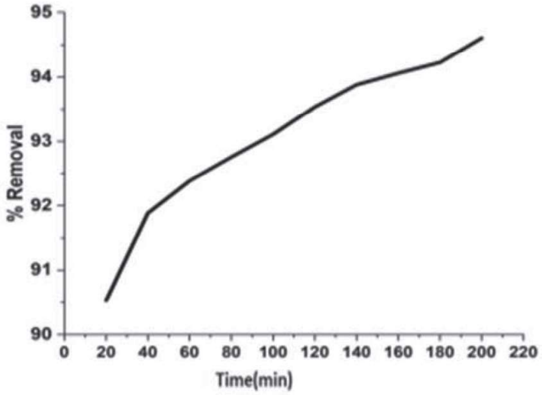

Fig.5(d) Effect of Contact Time

Effect Of Initial Metal Ion Concentration:

The study examined the capacity of the TRZCAC to bind Ni(II) at initial metal ion concentrations ranging from 10 ppm to 100 ppm.Due to the saturation of the biosorption sites at greater concentrations, the majority of the nickel is not absorbed.More binding sites are available at low metal ion concentrations. However, when the concentration increased, more ions competed for the limited number of binding sites in the biomass (Gupta & Mohapatra, 2003).

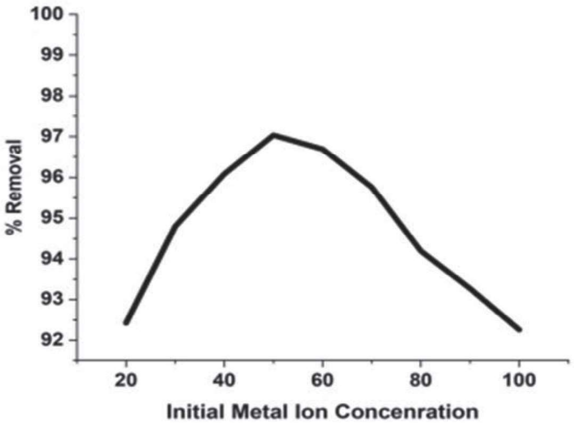

Fig 5(e): Effect of the Initial Metal Ions Concentration

Adsorption Isotherm:

Freundlich Adsorption Isothem:

The Freundlich adsorption isotherm model was found to be the best appropriate for the current investigation. To investigate the multilayer adsorption of the adsorbate (nickel ion) on the biosorbent (TRZCAC), the freundlich isotherm model is employed. The model can be used for a non-ideal sorption process with heterogeneous sites. The fundamental equation of the Freundlich Isotherm model is as follows.

$$Log\ q_e = \frac{1}{n} \ln C_e + \ln K_f \tag{3}$$

To calculate an object's adsorption capacity, utilize the Freundlich constant K_f and 1/n indicates how the adsorption process is favorable (0.1< 1/n < 0.5) or unfavorable (1/n > 2). R^2 was discovered to be equal to 0.99312, while the value of 1/n was discovered to be 0.3328, which denotes positive adsorption. **Table 1** displays the calculated parameter values for the Freundlich isotherm model. It is represented graphically in **Fig.6(a)**

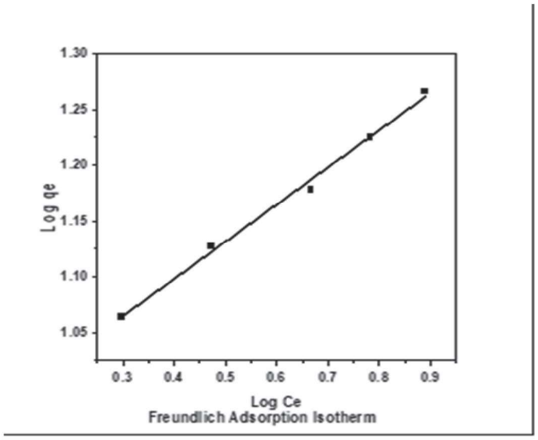

Fig 6(a): Langmuir Adsorption Isotherm

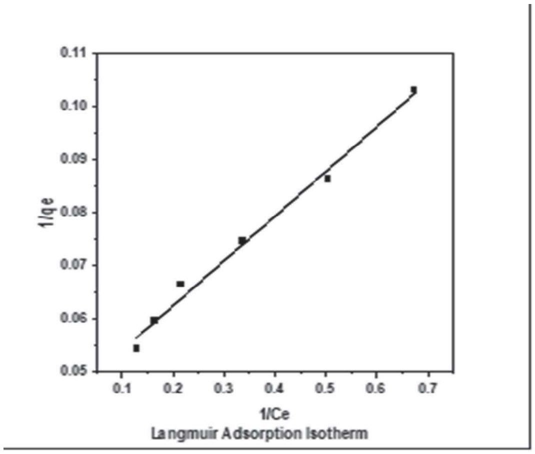

Fig.6(b):Freundlich Adsorption Isotherm

The Langmuir Adsorption Isotherm:

The Langmuir Isotherm model states that adsorption occurs on particular homogenous sites via a monolayer adsorption process, meaning that adsorption cannot occur there again once an adsorbate has occupied a site that is open to adsorption. On the other hand, the Langmuir isotherm model can be defined using the following equation:

$$\frac{Ce}{qe} = \frac{Ce}{qmax} + \frac{1}{b\ qmax} \qquad (4)$$

The equilibrium constant is b(L/mg), the equilibrium concentration of nickel adsorbed at equilibrium is Ce(mg/L), and the maximum adsorption capacity is indicated by qmax(mg/g). In Fig. 6(b), it is shown visually.The predicted values of the Langmuir adsorption isotherm are displayed in Table 1.

Types of Isotherm	Parameters	TRZCAC
Langmuir	q_{max}(mg/g)	21.97
	K_L(L/mg)	0.5390
	R_L	0.0357
	R^2	0.9875
Freundlich	K_f	9.2308
	1/n	0.3328
	R^2	0.9931

Table 1. Adsorption Isotherm parameter

Kinetic Models

Pseudo first order and Pseudo second order kinetics have been used to describe the kineic study(Long et al., 2018)(S. Kumar et al., 2014). In order to build an effective adsorption system and measure time-dependent variations in bioadsorption. It is necessary to utilize an appropriate kinetic model, which can only be done by studying the adsorption kinetics.

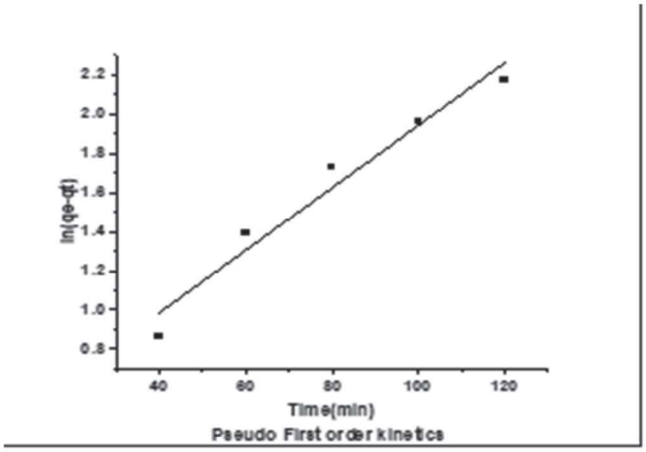

Fig 6(c):Pseudo first-order kinetics

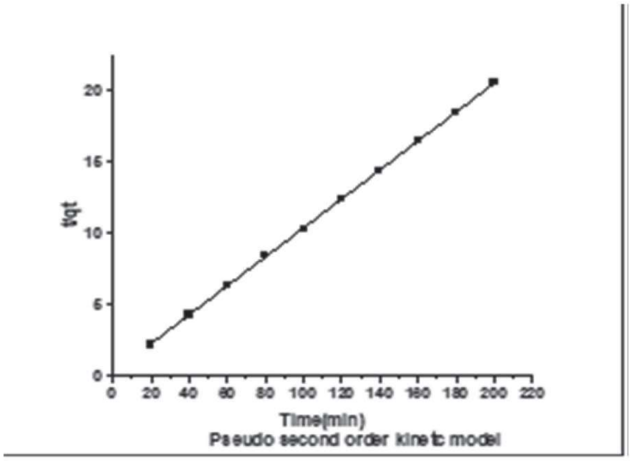

Fig 6(d): Pseudo second-order kinetics

$$\ln(qe - qt) = lnqe - K1t \tag{5}$$

where K_1 is the pseudo-first-order bioadsorption rate constant, and qe (mq/g) and qt (mg/g) are the adsorption capacities at equilibrium and time t, respectively. Graphing log (qe− qt) against time produces K1 and qe, correspondingly, based on the intercept and slope.

In order to explain metal ions adsorption onto adsorbents, Lagergran and Venska (1898) created the pseudo-second-order kinetic expression. The expression for the rate is as follows:

$$\frac{t}{qe} = \frac{1}{K2q2e} + \frac{1}{qe} \tag{6}$$

where K_2 (g/mg''min"1) is the rate constant for the pseudo-second-order adsorption reaction and q_e and q_t (mg/g) stand for the biosorption capacities at equilibrium and time t, respectively

It was demonstrated that a more accurate description of the Ni(II) metal ion adsorption on TRZCAC was provided by a pseudo-second-order kinetic model. because the linear regression coefficient (R^2 = 0.992) is higher. As depicted in **Table 2**. It suggests that the process by which Ni(II) metal ions bind onto TRZCAC is called chemisorption.

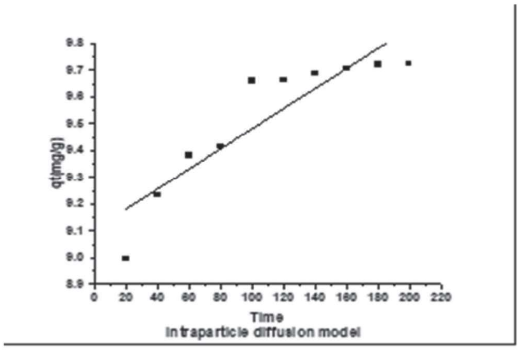

Fig 6(e): Intraparticle diffusion model

Table 2. Kinetic Parameters:

Order of Reaction	**Parameters**	**TRZCAC**
Pseudo first-order	K_1 (min^{-1})	-1.330 x 10-4
	R^2	0.94632
Pseudo second-order	K_2 (g mg^{-1} min^{-1})	0.0389
	R^2	0.992
Intrapartical diffusion	K_{int} (mg g^{-1}min$^{1/2}$)	0.00375
	$R^{2.}$	0.7926

Thermodynamics of Adsorption

Thermodynamics is essential for adsorption research since it relates the temperature to the kinetic energy of the metal ions in the solution. The rate at which metal ions diffuse into the biosorbent generally rises with temperature. The initial 50 mg/L concentration of Ni(II) ions bioadsorbed on TRZCAC at each of its ideal pH, TRZCAC dose, and Four different temperatures were studied for the equilibrium time values: 298 K, 303 K, 308 K, and 313 K.Temperature variations have an effect on the thermodynamic quantities, which are the enthalpy (ΔH°), entropy (ΔS°), and free energy.

The following formulas can be used to assess a change in biosorption:

$$\Delta G^0 = -RT \ln Kd \tag{7}$$

where K_d is the equilibrium constant, R is the gas constant (8.314 J/mol/K), and T is the temperature (K).

Table 3 demonstrates the spontaneous character of the reaction since the ΔG^{o} values are negative across the whole temperature range examined. The bioadsorption is proven to be exothermic as indicated by the negative value of ΔH° ($-$ 8.05 kJ/mol). The positive ΔS° value of 38.85 kJ/mol indicates the adsorbents' affinity for the Ni(II) ions.

The Van't Hoff Equation is used to get the entropy values. This is represented by enthalpy changes and Eq. (8).

$$\ln K = \left(\frac{\Delta S_0}{R}\right) - \left(\frac{\Delta H_0}{RT}\right) \tag{8}$$

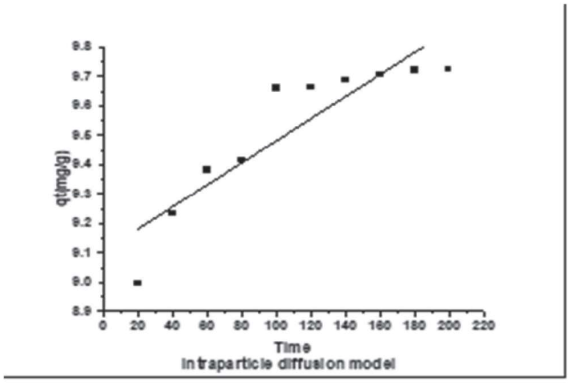

Fig 6(f): Van't Hoff plot

Table 3: Thermodynamic parameter:

Parameters	Temperature	TRZCAC
ΔG (K Jmol^{-1})	298 K	-3.75
	303 K	-4.06
	308 K	-4.25
	313 K	-4.56
ΔH (K J mol^{-1})		-8.05
ΔS (J mol^{-1} K^{-1})		38.85

Conclusion

In this study, the inexpensive and readily accessible Tabeubea rosea leaves powder are used as a biosorbent to eliminate nickel ions Ni (II) that have been activated with zinc chloride from an aqueous solution. Nitrogen adsorption-desorption analysis revealed a significant surface area of 693.113 m^2/g and a pore volume of 3.94 cm^3/g, indicating a highly porous structure suitable for adsorption.FT-IR spectra identified various functional groups present in TRZCAC, including O-H, -NH, aliphatic C-H, C-C stretching vibration of alkyne groups, carbonyl (carboxylic), N-H bending vibration, and phosphate functional groups.SEM examination showed well-defined porosity and an uneven surface with tunnel-like structures, advantageous for metal ion adsorption.Energy-dispersive X-ray spectroscopy confirmed the presence of carbon, oxygen, and other elements on the surface, with carbon and oxygen being the predominant constituents. Thermal gravimetric analysis demonstrated three stages of weight loss with increasing temperature, indicating the removal of water and volatile chemicals, decomposition of organic components, and carbon formation, suggesting carbon optimization for improved adsorption performance.According to the kinetic studies, after the adsorbate and adsorbent were in contact for 120 minutes at a swirling speed of 180 rpm, The equilibrium state for nickel ion adsorption on TRZCAC was discovered.Furthermore, it was discovered that the pseudo-second-order model's adsorption kinetics fit the data more closely than the pseudo-first-order model's, as shown by the correlation coefficient value (R^2).The sorption of Ni (II) on zinc chloride activated Tabeubea rosea leaf powder conforms to the model of the Freundlich isotherm, suggesting multilayer adsorption, according to the sorption isotherm fitting study.It was determined that the maximal sorption capacity was 21.97 mg/g. Studies on thermodynamics indicated that a greater sorption temperature was preferable. The predicted thermodynamic parameters values suggested an exothermic, spontaneous adsorption mechanism. TRZCAC is also used as a potential bioadsorbent to remove other Heavy Metal.The current study advances wastewater treatment applications by offering a cost-effective, efficient, and environmentally friendly solution for removing heavy metal contaminants from wastewater streams. Its findings contribute to the ongoing efforts to address water pollution challenges and improve water quality for human and environmental health.Beyond heavy metal removal, exploring the potential of TRZCAC for other applications such as organic pollutant removal, dye adsorption, or pharmaceutical wastewater treatment could broaden its scope of use and practical relevance.

Acknowledgment

The authors thank Rashtrasant Tukadoji Maharaj Nagpur University, Nagpur, India, and Shivaji Education Society Amravati's Science College, Congress Nagar, Nagpur. This research is not being funded by any agency.

Data Availability Statement

The paper contains every relevant detail.

Conflict of Interest

No conflict of interest, according to the author.

References

[1] Ahmad, A., Al-Swaidan, H. M., & Alghamdi, A. H. (2015). Production of Activated Carbon from Raw Date Palm Fronds by ZnCl2 Activation Production of Activated Carbon from Raw Date Palm Fronds by ZnCl 2 Activation. In *J.Chem.Soc.Pak* (Vol. 37, Issue 06).

[2] Ahmaruzzaman, M., & Gupta, V. K. (2011). Rice husk and its ash as low-cost adsorbents in water and wastewater treatment. *Industrial and Engineering Chemistry Research*, *50*(24), 13589–13613. https://doi.org/10.1021/ie201477c

[3] Akinhanmi, T. F., Ofudje, E. A., Adeogun, A. I., Aina, P., & Joseph, I. M. (2020). Orange peel as low-cost adsorbent in the elimination of Cd (II) ion: kinetics, isotherm, thermodynamic and optimization evaluations. *Bioresources and Bioprocessing*, *7*(1). https://doi.org/10.1186/s40643-020-00320-y

[4] Al-Qodah, Z. (2006). Biosorption of heavy metal ions from aqueous solutions by activated sludge. *Desalination*, *196*(1–3), 164–176. https://doi.org/10.1016/j.desal.2005.12.012

[5] Alhogbi, B. G. (2017). Potential of coffee husk biomass waste for the adsorption of Pb (II) ion from aqueous solutions. *Sustai nable Chemistry and Pharmacy*, *6*, 21–25. https://doi.org/10.1016/j.scp.2017.06.004

[6] Amode, J. O., Santos, J. H., Md. Alam, Z., Mirza, A. H., & Mei, C. C. (2016). Adsorption of methylene blue from aqueous solution using untreated and treated (Metroxylon spp.) waste adsorbent:

equilibrium and kinetics studies. *International Journal of Industrial Chemistry*, *7*(3), 333–345. https://doi.org/10.1007 /s40090-016-0085-9

[7] Bakatula, E. N., Richard, D., Neculita, C. M., & Zagury, G. J. (2018). Determination of point of zero charge of natural organic materials. *Environmental Science and Pollution Research*, *25*(8), 7823–7833. https://doi.org/10.1007/s11356-017-1115-7

[8] Bellahsen, N., Varga, G., Halyag, N., Kertész, S., Tombácz, E., & Hodúr, C. (2021). Pomegranate peel as a new low-cost adsorbent for ammonium removal. *International Journal of Environmental Science and Technology*, *18*(3), 711–722. https://doi.org/10.1007/s13762-020-02863-1

[9] Bello, O. S., Adegoke, K. A., & Akinyunni, O. O. (2017). Preparation and characterization of a novel adsorbent from Moringa oleifera leaf. *Applied Water Science*, *7*(3), 1295–1305. https://doi.org/10.1007/s13201-015-0345-4

[10] Biswas, B. K., Inoue, K., Ghimire, K. N., Kawakita, H., Ohto, K., & Harada, H. (2008). Effective removal of arsenic with lanthanum (III)- and cerium (III)-loaded orange waste gels. *Separation Science and Technology*, *43*(8), 2144–2165. https://doi.org/10.1080/01496390802064075

[11] Bulgariu, D., & Bulgariu, L. (2012). Equilibrium and kinetics studies of heavy metal ions biosorption on green algae waste biomass. *Bioresource Technology*, *103*(1), 489–493. https://doi.org/10.1016/j.biortech.2011.10.016

[12] Buekers, J., De Brouwere, K., Lefebvre, W., Willems, H., Vandenbroele, M., Van Sprang, P., Eliat-Eliat, M., Hicks, K., Schlekat, C. E., & Oller, A. R. (2015). Assessment of human exposure to environmental sources of nickel in Europe: Inhalation exposure. *Science of the Total Environment*, *521–522*, 359–371. https://doi.org/10.1016/j.scitotenv.2015.02.092

[13] Buxton, S., Garman, E., Heim, K. E., Lyons-Darden, T., Schlekat, C. E., Taylor, M. D., & Oller, A. R. (2019). Concise review of nickel human health toxicology and ecotoxicology. *Inorganics*, *7*(7). https://doi.org/10.3390/inorganics7070089

[14] Chand, R., Watari, T., Inoue, K., Torikai, T., & Yada, M. (2009). Evaluation of wheat straw and barley straw carbon for Cr(VI) adsorption. *Separation and Purification Technology*, *65*(3), 331–336. https://doi.org/10.1016/j.seppur.2008.11.002

[15] Das, A., Bar, N., & Das, S. K. (2020). Pb (II) adsorption from aqueous solution by nutshells, green adsorbent: Adsorption studies, regeneration studies, scale-up design, its effect on biological indicator and MLR modeling. *Journal of Colloid and Interface Science*, *580*, 245–255. https://doi.org/10.1016/j.jcis.2020.07.017

[16] El-Azazy, M., El-Shafie, A. S., Issa, A. A., Al-Sulaiti, M., Al-Yafie, J., Shomar, B., & Al-Saad, K. (2019). Potato Peels as an Adsorbent for Heavy Metals from Aqueous Solutions: Eco-Structuring of a Green Adsorbent Operating Plackett-Burman Design. *Journal of Chemistry*, *2019*. https://doi.org/10.1155/201 9/4926240

[17] Fan, L., Luo, C., Sun, M., Li, X., Lu, F., & Qiu, H. (2012). Preparation of novel magnetic chitosan/graphene oxide composite as effective adsorbents toward methylene blue. *Bioresourc e Technology*. https://doi.org/10.1016/j.biortech.2012 h.02.067

[18] Fischer, L. A., Menné, T., & Johansen, J. D. (2005). Experimental nickel elicitation thresholds - A review focusing on occluded nickel exposure. *Contact Dermatitis*, *52*(2), 57–64. https://doi.org/10.1111/j.0105-1873.2005.00523.x

[19] Gebreslassie, Y. T. (2020). Equilibrium, Kinetics, and Thermodynamic Studies of Malachite Green Adsorption onto Fig (Ficus cartia) Leaves. *Journal of Analytical Methods in Chemistry*, *2020*. https://doi.org/10.1155/2020/7384675

[20] Gupta, R., & Mohapatra, H. (2003). Microbial biomass: An economical alternative for removal of heavy metals from waste water. *Indian Journal of Experimental Biology*, *41*(9), 945–966.

[21] Haber, L. T., Bates, H. K., Allen, B. C., Vincent, M. J., & Oller, A. R. (2017). Derivation of an oral toxicity reference value for nickel. *Regulatory Toxicology and Pharmacology*, *87*, S1–S18. https://doi.org/10.1016/j.yrtph.2017.03.011

[22] Hariharan, A., Harini, V., Sandhya, S., & Rangabhashiyam, S. (2023). Waste Musa acuminata residue as a potential biosorbent for the removal of hexavalent chromium from synthetic wastewater. *Biomass Conversion and Biorefinery*, *13*(2), 1297–1310. https://doi.org/10.1007/s13399-020-01173-3

[23] Hasija, V., Raizada, P., Singh, P., Verma, N., Khan, A. A. P., Singh, A., Selvasembian, R., Kim, S. Y., Hussain, C. M., Nguyen, V. H., & Le, Q. Van. (2021). Progress on the photocatalytic reduction

of hexavalent Cr (VI) using engineered graphitic carbon nitride. *Process Safety and Environmental Protection*, *152*, 663–678. https://doi.org/10.1016/j.psep.2021.06.042

[24] Kahu, S. S., Shekhawat, A., Saravanan, D., & Jugade, R. M. (2016). Two-fold modified chitosan for enhanced adsorption of hexavalent chromium from simulated wastewater and industrial effluents. *Carbohydrate Polymers*, *146*, 264–273. https://doi.org/10.1016/j.carbpol.2016.03.041

[25] Kumar, A., Wang, L., Dzenis, Y. A., Jones, D. D., & Hanna, M. A. (2008). Thermogravimetric characterization of corn stover as gasification and pyrolysis feedstock. *Biomass and Bioenergy*, *32*(5), 460–467. https://doi.org/10.1016/j.biombioe.2007.11.004

[26] Kumar, S., Bhanjana, G., Dilbaghi, N., & Umar, A. (2014). Multi walled carbon nanotubes as sorbent for removal of crystal violet. *Journal of Nanoscience and Nanotechnology*, *14*(9), 7054–7059. https://doi.org/10.1166/jnn.2014.9236

[27] Li, Z., Teng, T. T., Alkarkhi, A. F. M., Rafatullah, M., & Low, L. W. (2013). Chemical modification of imperata cylindrica leaf powder for heavy metal ion adsorption. *Water, Air, and Soil Pollution*, *224*(4). https://doi.org/10.1007/s11270-013-1505-5

[28] Long, J., Huang, X., Fan, X., Peng, Y., & Xia, J. (2018). Effective adsorption of nickel (II) with Ulva lactuca dried biomass: Isoth erms, kinetics and mechanisms. *Water Science and Technology*, *78*(1), 156–164. https://doi.org/10.2166/wst.2018.253

[29] Lian, Q., Islam, F., Ahmad, Z. U., Lei, X., Depan, D., Zappi, M., Gang, D. D., Holmes, W., & Yan, H. (2021). Enhanced adsorption of resorcinol onto phosphate functionalized graphene oxide synthesized via Arbuzov Reaction: A proposed mechanism of hydrogen bonding and π-π interactions. *Chemosphere*, *280* (April), 130730. https://doi.org/10.1016/j.chemosphere.2021.130730

[30] LIU, Z. rong, ZHOU, L. min, WEI, P., ZENG, K., WEN, C. xi, & LAN, H. hua. (2008). Competitive adsorption of heavy metal ions on peat. *Journal of China University of Mining and Technology*, *18*(2), 255–260. https://doi.org/10.1016/S1006-1266(08)60054-1

[31] Mahmood, T., Saddique, M. T., Naeem, A., Westerhoff, P., Mustafa, S., & Alum, A. (2011). Comparison of different methods for the point of zero charge determination of NiO. *Industrial and*

Engineering Chemistry Research, *50*(17), 10017–10023. https://doi.org/10.1021/ie200271d

[32] Oller, A. R., Oberdörster, G., & Seilkop, S. K. (2014). Derivation of PM10 size-selected human equivalent concentrations of inhaled nickel based on cancer and non-cancer effects on the respiratory tract. *Inhalation Toxicology*, *26*(9), 559–578. https://doi.org/10.3109/08958378.2014.932034

[33] Pavlić, B., Naffati, A., Hojan, T., Vladić, J., Zeković, Z., & Vidović, S. (2017). Microwave-assisted extraction of wild apple fruit dust—production of polyphenol-rich extracts from filter tea factory by-products. *Journal of Food Process Engineering*, *40*(4), 1–11. https://doi.org/10.1111/jfpe.12508

[34] Raval, N. P., Shah, P. U., & Shah, N. K. (2016). Adsorptive removal of nickel(II) ions from aqueous environment: A review. *Journal of Environmental Management*, *179*, 1–20. https://doi.org/10.1016/j.jenvman.2016.04.045

[35] Rengaraj, S., Joo, C. K., Kim, Y., & Yi, J. (2003). Kinetics of removal of chromium from water and electronic process wastewater by ion exchange resins: 1200H, 1500H and IRN97H. *Journal of Hazardous Materials*, *102*(2–3), 257–275. https://doi.org/10.1016/S0304-3894(03)00209-7

[36] Sari, A., Tuzen, M., Citak, D., & Soylak, M. (2007). Equilibrium, kinetic and thermodynamic studies of adsorption of Pb(II) from aqueous solution onto Turkish kaolinite clay. *Journal of Hazardous Materials*, *149*(2), 283–291. https://doi.org/10.1016/j.jhazmat.2007.03.078

[37] Sharma, A., & Bhattacharyya, K. G. (2005). Adsorption of chromium (VI) on azadirachta indica (Neem) Leaf Powder. *Adsorption*. https://doi.org/10.1007/s10450-005-4818-x

[38] Sharma, Y. C., Singh, B., Agrawal, A., & Weng, C. H. (2008). Removal of chromium by riverbed sand from water and waste water: Effect of important parameters. *Journal of Hazardous Mat-erials*, *151*(2–3), 789–793. https://doi.org/10.1016/j.jhazmat.2007.06.054

[39] Song, C., Wu, S., Cheng, M., Tao, P., Shao, M., & Gao, G. (2014) (2014). Adsorption studies of coconut shell carbons prepared by KOH activation for removal of lead(ii) from aqueous solutions.

Sustainability (Switzerland), *6*(1), 86–98. https://doi.org/10.3390/su6010086

[40] Tsuji, M. (2002). SeO32--selective properties of inorganic materials synthesized by the soft chemical process. *Solid State Ionics*, *151*(1–4), 385–392. https://doi.org/10.1016/S0167-2738(02)00544-1

[41] Villaescusa, I., Fiol, N., Martínez, M., Miralles, N., Poch, J., & Serarols, J. (2004). Removal of copper and nickel ions from aqueous solutions by grape stalks wastes. *Water Research*, *38*(4), 992–1002. https://doi.org/10.1016/j.watres.2003.10.040

[42] Vinod, V. T. P., Sashidhar, R. B., & Sreedhar, B. (2010). Biosorption of nickel and total chromium from aqueous solution by gum kondagogu (Cochlospermum gossypium): A carbohydrate biopolymer. *Journal of Hazardous Materials*, *178*(1–3), 851–860. https://doi.org/10.1016/j.jhazmat.2010.02.016

[43] Vithalkar, S., Jugade, R. M., & Saravanan, D. (2022). Adsorption of brilliant green dye by used-tea-powder: equilibrium, kinetics and thermodynamics studies. *Aqua Water Infrastructure, Ecosystems and Society*, *71*(10), 1148–1158. https://doi.org/10.2166/aqua.2022.076

[44] Weber, C. T., Foletto, E. L., & Meili, L. (2013). Removal of tannery dye from aqueous solution using papaya seed as an efficient natural biosorbent. Water, Air, and Soil Pollution, 224(2). https://doi.org/10.1007/s11270-012-1427-7

[45] Yang, H., Yan, R., Chen, H., Lee, D. H., & Zheng, C. (2007). Characteristics of hemicellulose, cellulose and lignin pyrolysis. *Fuel*, *86*(12–13), 1781–1788. https://doi.org/10.10 16/j.fuel.2006.12.013

[46] Zhou, Y., Gao, B., Zimmerman, A. R., Fang, J., Sun, Y., & Cao, X. (2013). Sorption of heavy metals on chitosan-modified biochars and its biological effects. *Chemical Engineering Journal*, *231*, 512–518. https:/doi.org/10.1016/j.c ej.2013.07.036